



Published in final edited form as:

Neuroimage. 2016 May 01; 131: 29–41. doi:10.1016/j.neuroimage.2015.11.031.

Running rewires the neuronal network of adult-born dentate granule cells

Carmen Vivar¹, Benjamin D. Peterson, and Henriette van Praag*

Neuroplasticity and Behavior Unit, Laboratory of Neurosciences, Intramural Research Program, National Institute on Aging, National Institutes of Health, Baltimore, MD 21224, United States

Abstract

Exercise improves cognition in humans and animals. Running increases neurogenesis in the dentate gyrus of the hippocampus, a brain area important for learning and memory. It is unclear how running modifies the circuitry of new dentate gyrus neurons to support their role in memory function. Here we combine retroviral labeling with rabies virus mediated trans-synaptic retrograde tracing to define and quantify new neuron afferent inputs in young adult male C57Bl/6 mice, housed with or without a running wheel for one month. Exercise resulted in a shift in new neuron networks that may promote sparse encoding and pattern separation. Neurogenesis increased in the dorsal, but not the ventral, dentate gyrus by three-fold, whereas afferent traced cell labeling doubled in number. Regional analysis indicated that running differentially affected specific inputs. Within the hippocampus the ratio of innervation from inhibitory interneurons and glutamatergic mossy cells to new neurons was reduced. Distal traced cells were located in sub-cortical and cortical regions, including perirhinal, entorhinal and sensory cortices. Innervation from entorhinal cortex (EC) was augmented, in proportion to the running-induced enhancement of adult neurogenesis. Within EC afferent input and short-term synaptic plasticity from lateral entorhinal cortex, considered to convey contextual information to the hippocampus was increased. Furthermore, running upregulated innervation from regions important for spatial memory and theta rhythm generation, including caudo-medial entorhinal cortex and subcortical medial septum, supra- and medial mammillary nuclei. Altogether, running may facilitate contextual, spatial and temporal information encoding by increasing adult hippocampal neurogenesis and by reorganization of new neuron circuitry.

Keywords

Adult neurogenesis; Entorhinal cortex; Exercise; Hippocampus; Neural circuitry; Rabies virus; Retrograde tracing; Retrovirus

*Corresponding author at: Neuroplasticity and Behavior Unit, Laboratory of Neurosciences, NIA/NIH, Biomedical Research Center, Suite 100, 251 Bayview Blvd., Baltimore, MD 21224, United States. vanpraagh@mail.nih.gov (H. van Praag).

¹Present address: Laboratory of Neurogenesis and Neuroplasticity, Department of Physiology, Biophysics and Neuroscience, Centro de Investigación y de Estudios Avanzados del IPN, Mexico City, Mexico.

Introduction

Human and animal research indicates that exercise benefits brain function throughout the lifespan. In adult humans, spatial memory, working memory, and processing speed are improved by exercise (Voss et al., 2013), and in children academic achievement is enhanced (Donnelly et al., 2009). Furthermore, both epidemiological and intervention studies in aging subjects indicate that exercise may delay or prevent the onset of Alzheimer's disease (Larson et al., 2006; Lautenschlager et al., 2008). Research shows that the hippocampus, a brain area important for spatial navigation and memory formation (Buzsáki and Moser, 2013), is substantially modulated by physical activity (Voss et al., 2013). In humans, exercise increases hippocampal volume and vascularization (Erickson et al., 2011; Pereira et al., 2007; Maass et al., 2015). In rodents, multiple running-induced changes have been observed in the hippocampus (Vivar et al., 2013). Specifically, hippocampal neurotransmitter, neurotrophin levels, neuronal spine density, synaptic plasticity, angiogenesis and adult neurogenesis are increased with running (Voss et al., 2013; Sleiman and Chao, 2015; Patten et al., 2015).

In the hippocampus, the dentate gyrus subfield is considered to be particularly important for pattern separation, the processing of similar incoming information into distinct events and experiences (Marr, 1971; Treves et al., 2008; Yassa and Stark, 2011). New dentate granule cell neurons (Altman and Das, 1965; Eriksson et al., 1998) that become functionally integrated into the hippocampal circuitry (van Praag et al., 2002; Vivar et al., 2012) are considered to contribute to fine discrimination processes (Sahay et al., 2011a). Deficient adult neurogenesis impairs the ability to distinguish between closely related stimuli (Clelland et al., 2009; Guo et al., 2011; Tronel et al., 2012), whereas running-induced and transgenic elevation of neurogenesis enhance the ability to differentiate between similar stimuli (Creer et al., 2010; Sahay et al., 2011b; Bolz et al., 2015). However, whether such cognitive improvements can be attributed solely to a local increase in neurons is unclear. Lesion of perirhinal-lateral entorhinal cortex (PRH-LEC), a major input to new neurons, reduces performance on a high interference task in a touchscreen (Vivar et al., 2012). In addition, discrimination deficits result from silencing of synaptic transmission of adult-born neurons onto area CA3 (Nakashiba et al., 2012). Furthermore, new neuron ablation impairs area CA3 contextual encoding processes (Niibori et al., 2012). Thus, running-induced enhancement of mnemonic tasks may result from modifications in new neuron networks in conjunction with elevated levels of neurogenesis.

To begin to address this issue we analyzed the effects of voluntary wheel running on the afferent circuitry of new neurons. The majority of projecting cells were located in the entorhinal cortex. Running increased entorhinal input to new neurons, in proportion to the enhanced neurogenesis. In particular, lateral entorhinal cortex innervation and paired-pulse facilitation of lateral perforant pathway synapses onto new neurons was enhanced by running, which may support pattern separation in the dentate gyrus. Furthermore, running upregulated caudomedial entorhinal cortex inputs, considered to convey temporal and spatial information to the hippocampus. Concurrently, subcortical monosynaptic input from medial mammillary nucleus and supramammillary nucleus, while few in cell number, showed a striking elevation (~13-fold). Innervation from medial septum was enhanced proportionate to

the elevated neurogenesis. Our research shows that running recruits input to new hippocampal neurons from distal brain areas relevant to contextual and spatial–temporal information processing, and the genesis of the hippocampal theta rhythm. Overall, effects of running on the brain go beyond increased hippocampal neurogenesis, to modifications of cortical and subcortical brain regions that comprise the circuitry of new neurons.

Materials and methods

Animals

Male C57Bl/6 mice (Jackson Labs) 5–6 weeks old ($n = 69$) were individually housed and randomly assigned to control or voluntary wheel running conditions. Exercise animals were provided with a silent spinner running wheel (11.5 cm dia.). Running distance was monitored as described previously (Creer et al., 2010). Mice were housed in 12 h light–dark cycle (lights on at 6:00 a.m. and off at 6:00 p.m.) with food and water ad libitum. Animals were maintained according to the National Institute of Health guidelines, and protocols for procedures were approved by the NIA Institutional Animal Care and Use Committees.

Viral vector production

Retroviral vector RV-SYN-GTRgp, expressing nuclear green fluorescent protein (GFP), avian TVA receptor and rabies virus glycoprotein (Rgp) driven by the neuron-specific synapsin promoter, retroviral vector CAG-GFP and EnvA-pseudotyped rabies virus (EnvA-G-MCh) were produced as previously described (van Praag et al., 2002; Zhao et al., 2006; Wickersham et al., 2007; Vivar et al., 2012). Specifically, retrovirus was produced by transient transfection (Lipofectamine 2000, Invitrogen) of vector (7.5 μg), CMV-GagPol (5 μg) and CMV-VSVG (2.5 μg) in 90% confluent 293T cells. Virus-containing supernatant was harvested 36 h later filtered and concentrated by ultracentrifugation. Virus titers were estimated to be $\sim 1 \times 10^8$ i.u. ml^{-1} by serial dilution into 293T cells. To generate EnvA-pseudotyped gp-mCherry rabies virus (EnvA-G-MCh) glycoprotein-gene-deleted rabies virus vector (gp-mCherry) was used in which a mCherry (MCh) reporter gene was inserted into the locus encoding the rabies virus glycoprotein (provided by Dr. E. Callaway, Salk Institute). The helper cell line, BHK-EnvARGCD, was infected with gp-mCherry, to produce rabies virus pseudotyped with envelope protein EnvA. Supernatants containing gp-mCherry rabies virus pseudotyped with EnvA were harvested 5 days later, filtered and concentrated by ultracentrifugation. Rabies virus titer was estimated to be $\sim 1.2 \times 10^7$ i.u. ml^{-1} and diluted for use to $\sim 4 \times 10^6$ i.u. ml^{-1} .

Stereotaxic surgery

After three days of housing in their respective conditions, mice were anesthetized (Avertin 0.4 mg g^{-1} i.p.) and stereotaxic surgery was performed to deliver 1 μl of retrovirus RV-SYN-GTRgp or CAG-GFP into the right dorsal and ventral dentate gyrus (DG) using spatial coordinates relative to Bregma as follows: Dorsal DG, anterior–posterior (AP) = -2.10 mm; medial–lateral (ML) = 1.9 mm; dorso-ventral (DV) = -2.10 mm, and ventral DG, AP = -3.10 mm; ML = 2.8 mm; DV = -3.10 mm. These coordinates were modified from the mouse brain atlas (Paxinos and Franklin, 2007) and adjusted for mice aged 5–6 weeks at the time of the retroviral injection. For electrophysiological recordings from newborn neurons

CAG-GFP injected mice were sacrificed one month later to obtain acute hippocampal slices. For tracing experiments RV-SYN-GTRgp injected mice were anesthetized (Avertin 0.4 mg g⁻¹ i.p.) thirty days later and rabies virus EnvA- G-MCh (1 µl) was delivered into the same locations (Fig. 1A, B). One week later animals were given an overdose of isoflurane anesthetic (Abbott) and perfused transcardially with 0.9% saline at RT followed by cold 4% paraformaldehyde in 0.1 M PBS. After post-fixation for 24 h, brain tissue was equilibrated in 30% sucrose. Sequential horizontal sections (40 µm) were taken using a freezing microtome (HM450, ThermoFisher) through the dorsal ventral extent of the brain and stored in phosphate-buffer glycerol at -20 °C.

Immunohistochemistry and cell counts

To identify and quantify the brain areas and the cell types providing inputs to the newborn GCs, analysis of the dual-infected (retrovirus and rabies virus) starter cells (SC) expressing both GFP and MCh in the dentate gyrus, and the traced cells (TC) expressing only MCh throughout the brain, was carried out in a 1:6 series (240 µm apart) of horizontal sections (40 µm) through the dorso-ventral extent of the brain. Sections were stained for GFP (chicken polyclonal, 1:1000, Aves Labs) and corresponding fluorescent secondary antibody (donkey anti-chicken Alexa Fluor 488, 1:250, JacksonImmunoResearch) using 40-µm free-floating sections as described (Creer et al., 2010). Nuclei were visualized with 4'-6-diaminodino-2-phenylindole (DAPI).

DG starter cells—To quantify the number of starter cells (SC, GFP⁺ and MCh⁺), and traced cells (TC, MCh⁺ only) in the DG, confocal images (FV 1000MPE, Olympus), fifteen to eighteen z-planes at 1 µm intervals, were taken at 20×. Only mouse brains with 65% or more double-labeled cells (GFP⁺-MCh⁺) from the total number of GFP⁺ cells in the DG were taken for tracing analysis (6 of 11 of the control group, and 7 of 9 of the running group).

Hippocampal traced cells—Mature granule cells (mGCs) and interneurons (INT) in the DG were identified based on location and morphology. The granule cell neurons have an elliptical cell body localized in the granule cell layer (GCL) and characteristic cone-shaped tree of spiny apical dendrites. Granule cells were cataloged as mature (mGCs) if they expressed MCh only, as described previously (Vivar et al., 2012). Interneurons (INT) were identified in the DG based on the location of their somata as follows: 1) INT of the molecular layer (INT-ML) if the soma was positioned in the ML INT-ML (also called MOPP cells) (Han et al., 1993) typically have a fairly round soma with two major dendrites emerging from the cell body, that give rise to several secondary dendrites fanning out radially into the ML. 2) INT of the GCL if the soma was localized in the GCL-hilus border (INT-GCL), and expressing MCh only. INT-GCL are a mix of basket cells, axo-axonic cells and HIPP and HICAP cells (Freund and Buzsáki, 1996). Basket cells are characterized by a pyramidally-shaped soma with a prominent apical dendrite emerging from the soma. Their basal dendrites (2–5) enter the hilus. Axo-axonic cells typically have a dendritic tree with a tuft of several radially running branches. HIPP cells have a large fusiform soma which branches profusely developing into the dendritic tree. HICAP cells typically have a triangular cell body and the primary dendrites have a multipolar origin. INT in the CA areas

were also identified by their morphology. These cells have an elliptical soma and several long primary dendrites that often stretch parallel to the pyramidal cell layer before giving rise to several secondary dendrites. CA INT are located in the stratum oriens and stratum lucidum, as well as on the borders of the pyramidal cell layer. In addition, immunostaining was performed for GABA (rabbit polyclonal, 1:500, Sigma) with secondary donkey anti-rabbit Alexa Fluor 488 (1:250, JacksonImmunoResearch) in additional sections to determine co-localization with MCh. Mossy cells (MC) were identified by their location in the hilus of the DG, their characteristic morphology with thorny excrescences covering the proximal ends of their long, thick dendritic branches (Blasco-Ibañez and Freund, 1997). An additional set of sections was stained for the mossy cell marker calretenin (goat polyclonal, 1:1000, Millipore) with donkey anti-goat Alexa Fluor 488 (1:250, JacksonImmunoResearch) as a secondary antibody.

Dorso-ventral distribution analysis—For the analysis of the dorso-ventral distribution of SC and hippocampal TC [(mature granule cells (mGCs), interneurons (INT), pyramidal cells (PYR), mossy cells (MC)], the entire hippocampus was divided in dorsal, middle and ventral regions. Dorsal hippocampus: -1.24 mm to -2.16 mm from Bregma. Middle hippocampus: -2.36 mm to -2.96 mm from Bregma. Ventral hippocampus: -3.16 mm to -4.12 mm from Bregma. Total number of SC or TC was calculated by region (dorsal, middle and ventral) and compared between control and running groups.

Distal cortical and sub-cortical traced cells and regional analysis—To evaluate the traced cells (TC) expressing MCh entire sections were imaged at $4\times$ using a fluorescent microscope (BX51, Olympus). Sections were reconstructed by stitching the images using CorelDraw. After reconstruction, sections were matched to the mouse brain atlas (Paxinos and Franklin, 2007) to determine the dorso-ventral depth (distance from Bregma). Next, higher magnification images were taken ($10\times$ objective, BX51, Olympus) to allow for detailed quantification of TC. Cells were classified and counted by experimenters who were blinded to group identity of the samples, in their respective dorso-ventral depth (distance from Bregma) based on the mouse brain atlas (Paxinos and Franklin, 2007) throughout the dorso-ventral extent of the brain. Entorhinal cortex (EC) cells were determined to be in the lateral entorhinal cortex (LEC), perirhinal cortex (PRH), medial entorhinal cortex (MEC) and caudo-medial entorhinal cortex (CEnt) using defined parameters (Dolorfo and Amaral, 1998; van Groen, 2001). Total cell numbers were obtained by multiplying by six. Photomicrographs for the figures were prepared utilizing parallel series of sections from the same brains used for quantitative analysis. For Figs. 3A,F,G and 5 sections were double-labeled for GFP (chicken polyclonal, 1:1000, Aves Labs) and red fluorescent protein (rabbit polyclonal, 1:1000, Rockland) and corresponding fluorescent secondary antibodies (donkey anti-chicken Alexa Fluor 488, 1:250; donkey anti-rabbit CY3, 1:250, Jackson ImmunoResearch). Images were taken with confocal microscopy (FV 1000MPE, Olympus) and z-series were merged and processed using Slidebook (Intelligent Imaging Innovations) and Photoshop (Adobe).

BrdU injections and histology

Bromodeoxyuridine (BrdU, Sigma) was dissolved in 0.9% NaCl and filtered sterile. Control ($n = 5$) and runner ($n = 5$) mice received single daily doses of 50 $\mu\text{g/g}$ body weight at a concentration of 10 mg/ml intra-peritoneally (i.p.) for 4 days, starting the day after individual housing. One month after the last injection mice were given an overdose of isoflurane anesthetic (Abbott) and perfused transcardially as described above.

BrdU immunohistochemistry and cell counts—BrdU⁺ cell number was counted as described previously (Creer et al., 2010). To determine the number and distribution of BrdU⁺ cells, a 1:6 series of equidistant horizontal sections (240 μm apart) were stained (rat anti-BrdU, 1:100, Accurate Chemical) using the peroxidase method [ABC system, with biotin-SP conjugated donkey anti-rat (1:250, Jackson ImmunoResearch), and 3,3'-diaminobenzidine (DAB) as a chromogen, Vector Laboratories]. BrdU⁺-DAB cells in the DG were imaged and counted through a 20 \times objective (BX51, Olympus). Analysis of the dorso-ventral distribution of the BrdU⁺ cells throughout the extent of the DG was based on the distance below Bregma in the mouse brain atlas (Paxinos and Franklin, 2007).

Electrophysiology

Twenty-eight to 35 days after CAG-GFP virus injection, mice were anesthetized with isoflurane and decapitated. Brains were removed into a chilled solution containing (in mM): 110 Choline-Cl, 2.5 KCl, 2 NaH₂PO₄, 25 NaHCO₃, 20 glucose, 0.5 CaCl₂, 7 MgCl₂, 0.6 Na⁺ pyruvate, 1.3 Na⁺ ascorbate, and 1 kynurenic acid. Horizontal cortico-hippocampal slices (350 μm thick) were obtained and transferred to a chamber containing artificial cerebrospinal fluid (ACSF) in mM: 125 NaCl, 2.5 KCl, 2 NaH₂PO₄, 25 NaHCO₃, 2 CaCl₂, 1.3 MgCl₂, 10 glucose, 3.1 Na⁺ pyruvate, 1.3 Na⁺ ascorbate, bubbled with 95% O₂/5% CO₂ (pH 7.4, 310 mOsm). Slices were incubated at 30 °C for 30 min and stored at room temperature afterwards. Recordings were carried out in ACSF at 28 \pm 1 °C using microelectrodes (3–5 M Ω) pulled from borosilicate glass (G150F-4, Warner Instruments). For recording of mIPSCs, pipettes were filled with (in mM): 140 CsCl, 5 NaCl, 4 MgCl, 0.1 EGTA, 10 HEPES, 4 Na-ATP, 0.3 Na-GTP, 10 Na-phosphocreatine and 5 lidocaine N-ethyl bromide (QX-314) (pH 7.3, 294 mOsm). For recording of mEPSCs, EPSCs and intrinsic properties pipettes were filled with (in mM): 120 K-gluconate, 20 KCl, 5 NaCl, 4 MgCl₂, 0.1 EGTA, 10 HEPES, 4 Tris-ATP, and 10 phosphocreatine (pH 7.4, 295 mOsm). mIPSCs were recorded in presence of 1 μM tetrodotoxin (TTX), 10 μM of D-2-amino-5-phosphonopentanoic acid (D-AP5) and 10 μM of 2,3-dioxo-6-nitro-1,2,3,4-tetrahydrobenzo (f) quinoxaline-7-sulfonamide (NBQX). mEPSCs were recorded in presence of 1 μM TTX and 20 μM bicuculline methiodide (BIC). Evoked EPSCs were recorded in presence of 20 μM BIC.

Newborn GCs were identified by expression of GFP under epifluorescence and visualized with infra-red differential interference contrast video microscopy (Olympus BX51WI). Mature GCs born during development (Nowakowski and Rakic, 1981) were recorded from the outer portion of the GC layer (mGCs-OGCL). Whole-cell patch-clamp recordings (Multiclamp 700B, Axon Instruments) were filtered at 2 kHz and digitalized at 20 kHz (Digidata 1322A and pClamp 10.2 Software; Molecular Devices). Series resistance was

typically 10–30 M Ω . Extracellular stimulation (10 μ s, 0.05 Hz; Grass S88 stimulator and isolation unit, Grass Instrument) was carried out using pipettes (2–4 M Ω) filled with ACSF placed in the middle third (MPP) and outer (LPP) molecular layer at >250 μ m from the recorded cell.

Data analysis—Miniature postsynaptic currents were detected and analyzed (peak amplitude, frequency, rise and decay time) offline using MiniAnalysis software (Synaptosoft). Minimum amplitude of synaptic currents for detection was set at 10 pA peak amplitude for mIPSCs and 5 pA for mEPSCs. All detected events were individually validated and artifacts were discarded by visual inspection. Analysis typically contained ~200 events for mIPSCs and ~100 events for mEPSCs per cell. A mean value was obtained for each cell and the resulting means were averaged between conditions. Intrinsic properties analysis: Rin was measured using a linear regression of voltage deflections (\pm 15 mV resting potential, \sim -75 mV) in response to 600 ms current steps of 6–10 different amplitudes (increments, 5 pA). AP amplitude was defined as the difference in membrane potential between threshold and the peak. After-hyperpolarization (AHP) amplitude was defined as the difference between AP threshold and the most negative membrane potential attained during the AHP. Firing frequency was calculated as the inverse of the mean inter-spike interval of the first two inter-spike intervals of the train. Paired-pulse ratio was defined as the peak amplitude of the EPSC2/EPSC1.

Statistical analysis

Statistical analyses were carried out using GraphPad Prism 5. Comparisons between control and running groups for histological data were performed with Student's *t*-test. The mIPSCs and mEPSCs experiments were analyzed using 2-way analysis of variance (ANOVA) and Fisher's PLSD post-hoc comparisons. Significance of the shift in cumulative probability distributions of amplitude and inter-event interval was assessed by pooling together the data of each experiment for each condition and using the non-parametric Kolmogorov–Smirnov two-sample test (KS test). All values were expressed as means \pm S.E.M.

Results

Combination of retro- and rabies virus to define monosynaptic inputs to new neurons

To determine how new neuron circuitry is altered by running we applied the EnvA–TVA tracing method (Wickersham et al., 2007). Specifically, Murine Moloney leukemia virus which only infects dividing cells (Lewis and Emerman, 1994) was modified to generate a retroviral vector (van Praag et al., 2002) expressing nuclear green fluorescent protein (GFP), avian TVA receptor and rabies virus glycoprotein (Rgp) driven by the neuron-specific synapsin promoter (Vivar et al., 2012). This retroviral vector (RV-SYN-GTRgp) was injected into the dorsal and ventral DG to label proliferating neural progenitor cells of control ($n = 6$) and runner ($n = 7$) mice (Fig. 1A, B). Running distance increased during the first week and then reached a plateau (see Inline Supplementary Fig. S1A). Following a thirty-day interval after retroviral injection, to allow the progenitor cells to mature into new neurons, EnvA-pseudotyped rabies virus lacking Rgp (EnvA- G-MCh), was injected into the same DG areas and mice were perfused one week thereafter. This rabies virus selectively infects new

neurons expressing the TVA receptor. These dual-infected cells are termed “starter cells” (SC). The SC co-express GFP and mCherry (MCh) and are the origin of the trans-synaptic tracing, as the rabies virus is complemented with Rgp provided by the retrovirus in the SC. The virus crosses synapses to presynaptic neurons, and because the traced cells lack Rgp, the virus does not spread any further, labeling only monosynaptic inputs (Vivar et al., 2012; Vivar and van Praag, 2013; Wickersham et al., 2007). Previous studies validated this method by demonstrating that there is no transsynaptic spread of rabies virus if the retrovirus lacks Rgp (Vivar et al., 2012) and that neuronal activity does not directly affect rabies virus transsynaptic transfer (Bergami et al., 2015). In the present study, histological analysis showed similar dual-virus labeling (GFP–MCh) in the SC of control (~86% of all GFP⁺ cells) and runner (~71% of all GFP⁺ cells) mice (see Inline Supplementary Fig. S1B). Traced cells (TC) expressing only MCh are the cells providing the SC with monosynaptic input.

Inline Supplementary Fig. S1 can be found online at <http://dx.doi.org/10.1016/j.neuroimage.2015.11.031>.

Running increases new granule cell (GC) number and total afferent input

Running significantly increased adult neurogenesis as reflected in elevated numbers of GFP⁺ cells (see Inline Supplementary Fig. S1C) and GFP⁺–MCh⁺ newborn SC (Fig. 1C–F). Dorso-ventral (septo-temporal) distribution analyses (see Inline Supplementary Fig. S2A) showed that running significantly elevated SC number in the dorsal, but not in the middle or ventral DG (Fig. 1G). Similarly, dorso-ventral analysis of the GFP⁺ cells (see Inline Supplementary Fig. S2B), as well as of bromodeoxyuridine (BrdU) labeled cells in a separate cohort of animals (BrdU, CON, $n = 5$; RUN, $n = 5$; Fig. 2), showed a running-induced increase in the dorsal DG, indicating regional differences in the neurogenic response to physical activity.

Exercise also significantly increased the total number of traced cells (Fig. 1H). The running-induced increase in total TC was ~2-fold, while that of the SC was ~3-fold (see Inline Supplementary Fig. S3). Consistently, calculation of the ratio of TC to SC showed a trend towards a reduction in runners in the proportion of TC to SC (~8:1 CON vs ~5:1 RUN; Fig. 1I), suggesting that running modifies new neuron circuitry. Subsequently, we analyzed TC within the hippocampal, distal sub-cortical and cortical regions.

Inline Supplementary Figs. S2 and S3 can be found online at <http://dx.doi.org/10.1016/j.neuroimage.2015.11.031>.

Running modifies intra-hippocampal afferents to the newborn GCs

Analysis of TC in the hippocampus showed that newborn GCs receive intra-hippocampal inputs from mature granule cells (mGC), pyramidal cells (PYR), interneurons (INT), mossy cells (MC), and subicular complex cells [subiculum (SUB), parasubiculum (PAR) and presubiculum (PRE)] (Fig. 3 and see Inline Supplementary Fig. S4). The number of traced mGC was significantly increased by running (Fig. 3B–E, H), but the proportion of traced mGC to newborn SC was unaltered (Fig. 3I). Dorso-ventral analysis showed that running significantly increased the quantity of traced mGCs in the dorsal DG, similar to the

distribution of the increase in new GCs (see Inline Supplementary Fig. S5). Running did not change the number of traced mossy cells (MC), but there was a substantial reduction in the ratio of traced MC to SC (Fig. 3H, I). This may be due to the limited number of MCs in the hippocampal formation (Blasco-Ibañez and Freund, 1997), most of which may already be incorporated into the new neuron circuitry under control conditions. We also analyzed traced MC contralateral to the side of the virus injection and found no significant changes in TC number (see Inline Supplementary Fig. S6). Furthermore, direct ‘back-projections’ from Cornu Ammonis (CA) areas CA3, CA2 and CA1 pyramidal cells (PYR) were observed in both control and runner mice (Fig. 3A, G–J). Of these, area CA3 traced PYR accounted for ~80% of the total traced PYR (Fig. 3J). Neither the total number nor the ratio of traced PYR to SC was modified by exercise (Fig. 3H, I), suggesting that there may be a specific subset of PYR providing direct input to the newborn GCs. Running did not modify the dorso-ventral distribution of area CA3, CA2 and CA1 PYR throughout the hippocampus (see Inline Supplementary Fig. S7).

Traced interneurons (INT) were localized in the molecular layer (ML) and granule cell layer (GCL) of the DG, and in areas CA3, CA2 and CA1, with the majority of traced INT in the GCL and area CA3 (Fig. 3A, F, K; see Inline Supplementary Fig. S8). Running did not alter the total number of traced interneurons (Fig. 3H) nor their dorso-ventral distribution throughout hippocampus (see Inline Supplementary Fig. S8). Exercise did significantly reduce traced INT to SC ratio (Fig. 3I), raising the possibility that newborn GCs may receive less inhibition. To evaluate the effect of running on GABAergic inhibitory transmission, recordings of miniature inhibitory postsynaptic currents (mIPSCs) were made. Neither the mean amplitude nor the frequency of mIPSCs of new GCs was modified by exercise (Fig. 4A, C, D, F). To test the effect of running on the population of GCs born during early development (Nowakowski and Rakic, 1981), mature granule cells in the outer part of the GCL (mGC-OGCL) were recorded. Analysis showed that the amplitude of mIPSCs of mGC-OGCL was elevated compared to new GCs (Fig. 4B, C). Moreover, the frequency of mIPSCs was increased by exercise (CON, $n = 10$ cells from 3 mice, RUN $n = 11$ cells from 3 mice), suggesting running evoked strong GABAergic inhibition onto mGC-OGCLs (Fig. 4B, E, F).

Inline Supplementary Figs. S4–S8 can be found online at <http://dx.doi.org/10.1016/j.neuroimage.2015.11.031>.

Subcortical connections to new GCs are modified by running

Retrograde tracing also revealed running-induced modifications in the synaptic inputs from distal subcortical areas such as the basal forebrain and mammillary bodies to the newborn GCs. Analysis of the basal forebrain showed that the total number of TC from medial septum (MS) was significantly increased, but not the ratio of traced MS cells to SC (Fig. 5A–E). In the diagonal band of Broca (DBB) the traced cell number was not affected by running and the ratio of traced DBB cells to SC was reduced (Fig. 5A,B). This suggests that DBB provides afferent innervation to newborn GCs from a limited number of cells. In addition to basal forebrain, retrograde tracing revealed afferents from medial mammillary bodies (MM) and supramammillary nuclei (SUM) pars lateralis (Fig. 5F–J). Strikingly, these

afferent inputs are greatly increased (~13-fold) with exercise, resulting in a significant increase in the ratio of SUM TC to SC and a trend towards an increase in the ratio of MM TC to SC (Fig. 5G). Indeed, these are the only brain regions that showed an elevated TC to SC ratio.

New neurons receive input from entorhinal, perirhinal and sensory cortices

The largest population of TC was localized in cortex. Sparse innervation from sensory cortices was observed. Traced cells were detected in the auditory, visual and somatosensory cortices, none of which differed in number between control and runner mice (see Inline Supplementary Fig. S9). The predominant input to new GCs was from entorhinal (EC) and perirhinal (PRH) cortex (Fig. 6). EC is the main excitatory cortical input to the DG (Knierim et al., 2013). Exercise significantly increased the total number of traced EC-PRH cells (Fig. 6A-D), but not the ratio of total traced EC-PRH to SC as compared to controls (~3:1; Fig. 6E). Within EC, the medial entorhinal cortex (MEC) is deemed to relay spatial-temporal information to the hippocampus, whereas lateral entorhinal cortex (LEC) is considered to convey information about the content and context of an experience (Knierim et al., 2013). In runners compared to controls, TC were increased in caudo-medial entorhinal cortex (CEnt), LEC and MEC but not the ratio of TC to SC (Fig. 6F,G; see Inline Supplementary Fig. S10).

Inline Supplementary Figs. S9 and S10 can be found online at <http://dx.doi.org/10.1016/j.neuroimage.2015.11.031>.

To evaluate glutamatergic transmission, recordings of miniature ex-citatory postsynaptic currents (mEPSCs) and measurements of short-term plasticity were performed (Fig. 7A-I). mEPSCs are the result of glutamatergic inputs, mainly from cortical neurons, but also from intra-hippocampal and subcortical neurons. Exercise significantly reduced the mean amplitude of mEPSCs of newborn GCs, whereas in mGC-OGCL the amplitude was increased (Fig. 7A-C). Exercise increased the mean frequency of mEPSCs of mGC-OGCL, while the frequency of newborn GCs was unchanged (Fig. 7A,B,D-F). To investigate the specific modifications to EC inputs, short-term plasticity was evaluated by paired-pulse stimulation of either lateral perforant pathway (LPP; input from LEC; Fig. 7G, H) or medial perforant pathway (MPP; input from MEC; Fig. 7G, I). Running significantly increased paired-pulse facilitation (PPF) evoked by stimulation of LPP, but not MPP in the new GCs (Fig. 7H, I). No changes were observed in paired-pulse stimulation of either LPP or MPP stimulation onto mGC-OGCL (Fig. 7H, I).

Discussion

Running-induced neurogenesis is considered to contribute to enhanced cognitive function. However, this improvement may not just depend on new neuron addition, but also on changes in their local hippocampal, distal subcortical and cortical networks. Running increases the number of starter cells by three-fold and traced cells by two-fold, modifying the organization of new neuron afferent circuitry. In addition, the overall ratio of traced cells to starter cells showed a trend towards a reduction in runners. These findings suggest that while the circuitry is expanded by running, convergence of inputs onto individual neurons may be reduced, which could be conducive to network stability, sparse activation, and

pattern separation. Running also differentially affected afferent brain areas. Within the hippocampus, input from mossy cells and interneurons was decreased relative to the running induced enhancement in adult neurogenesis. Inhibitory synaptic transmission onto the new neurons, however, was not changed, whereas developmentally born granule cells became strongly inhibited. Input from entorhinal cortex was increased proportionate to running-induced neurogenesis. However, only short-term synaptic plasticity from lateral entorhinal cortex, a brain area important for providing information about the content and context of experiences to the hippocampus, was enhanced. Interestingly, running also resulted in recruitment of inputs from several brain areas relevant to spatial–temporal information processing and genesis of the hippocampal theta rhythm (CEnt, MM, SUM, MS). Overall, the effects of running go beyond increased neurogenesis, by inducing changes in the new neuron physiology and circuitry that may contribute to improved brain function.

It is well-established that running increases adult hippocampal neurogenesis (van Praag et al., 1999a,b; van der Borght et al., 2007; Vivar et al., 2013; Voss et al., 2013; Patten et al., 2015). However, the regional distribution of running-induced changes is not as well characterized. Several different approaches, including retroviral labeling, dual retro- and rabies virus infection (starter cells) and BrdU labeling showed an increase in new cells mainly in the dorsal dentate gyrus. The mechanisms underlying the regional difference in neurogenic capacity are unclear. Previous studies have shown that, under control conditions, the dorsal aspect has a higher number and faster maturation rate of new neurons than the ventral dentate gyrus (Snyder et al., 2009; Jinno, 2011; Piatti et al., 2011; Lowe et al., 2015). Similar to our findings environmental enrichment including a running wheel (Tanti et al., 2012) and a recent running study using doublecortin labeling (Bolz et al., 2015) report increased dorsal dentate gyrus neurogenesis. The differential regulation of adult neurogenesis along the dorso-ventral (septo-temporal) axis may reflect functional differences between dorsally- and ventrally-born new neurons. Indeed, spatial processing is thought to rely on the dorsal hippocampus whereas the ventral hippocampus is considered relevant for regulation of emotions (Fanselow and Dong, 2010). Future studies may be needed to elucidate differences between dorsal and ventral circuitry to provide insight into the roles in cognition and depression (Sahay and Hen, 2007) attributed to new neurons.

Dorso-ventral differences were also observed in the traced cells. The input from mature granule cells (mGCs) to new neurons is increased by running commensurate to elevated neurogenesis in the dorsal DG. Indeed, mGCs appear to surround new neurons, forming clusters, raising the possibility that these mGCs may be older adult-born neurons. The mGCs could support subsequent generations of new neurons by providing the glutamatergic input necessary for activity-dependent maturation (Tashiro et al., 2006). Others suggest that labeling of mGCs reflects pseudotransduction (Deshpande et al., 2013). Although retroviral vectors can only stably integrate into the genome of dividing cells (Lewis and Emerman, 1994), a non-integrating viral infection may result in transgene expression (Haas et al., 2000), which could render non-proliferating cells susceptible to rabies virus infection. However, upon injection of retrovirus expressing GFP, TVA and Rgp into non-neurogenic cortex followed by EnvA- G-MCh rabies virus thirty days thereafter, no labeling was observed (data not shown), supporting our findings that new adult-born neurons receive input from mature granule cells (Vivar et al., 2012).

While the flow of information into hippocampus from cortex is generally considered to be propagated serially by excitatory synaptic transmission to DG → CA3 → CA1 and back to cortex (Amaral and Witter, 1989) it has become increasingly clear that there are recurrent networks (Lisman, 1999; Scharfman, 2007). Anatomical evidence shows that area CA3 pyramidal cells project back to the DG (Li et al., 1994) and provide direct input to new neurons (Vivar et al., 2012). These traced cells are located mainly in area CA3, followed by sparse input from area CA2 and CA1 pyramidal cells. The input from area CA1 is consistent with anatomical studies showing that their axons cross the hippocampal fissure to sparsely innervate the molecular layer of the DG and the hilus (Cenquizca and Swanson, 2007). Running did not modify the number of traced pyramidal cells or their ratio to starter cells, suggesting that there may be a specific subset of cells providing direct input to the newborn GCs. A direct back-projection from hippocampal pyramidal cells may play a role in the processing of sequential information, by correcting cumulative errors produced by the serial unidirectional propagation of cortical information (Lisman et al., 2005). Further research is needed to determine the specific role of these direct back-projections.

Traced interneurons were observed mainly in the granule cell layer, molecular layer and area CA3 and sparsely in areas CA2 and CA1. Running did not modify the traced interneuron number and significantly reduced their ratio to starter cells, possibly due to the small number of these neurons in the hippocampus, ~10% of the total hippocampal neural population (Freund and Buzsáki, 1996). A recent study reported, however, that six weeks of running did not change interneuron to starter cell ratio, suggesting a parallel running-induced increase in traced interneuron and new granule cells. Furthermore, environmental enrichment, including running wheels, increased the interneuron to starter cell ratio, indicating that the increase in quantity of traced inter-neurons exceeded new neuron number. Unfortunately, total traced cell numbers were not reported (Bergami et al., 2015), precluding direct comparisons with our study.

Interestingly, our results showed that although the ratio of interneuron input to new neurons was reduced, GABAergic inhibitory synaptic transmission measured by amplitude and the frequency of mIPSCs of new GCs was not changed by running. On the other hand, in mature GCs in the outer molecular layer (mGC-OGCL), considered to be born during development (Nowakowski and Rakic, 1981), synaptic inhibition was strongly increased, possibly due to interneuron sprouting of axonal collaterals onto these cells (Zhang et al., 2009) in runners. Such a process may underlie the proposed enhancement of sparse encoding by feedback inhibition mediated by hilar cells (McAvoy et al., 2015; Finnegan and Becker, 2015). Our results also provide insight into studies in which all mice were housed with running wheels (Schmidt-Hieber et al., 2004; Marín-Burgin et al., 2012; Temprana et al., 2015). In runners new neurons were easily activated by weak entorhinal input, whereas mGCs-OGCL required strong activation of entorhinal afferents. However, when GABAergic inhibition was blocked, mGC-OGCL were activated as easily as newborn neurons (Marín-Burgin et al., 2012). Similarly, upon activation of hilar interneurons mGC-OGCL are strongly inhibited, as compared to new neurons, in recordings in slices derived from running mice (Temprana et al., 2015). This suggests that increased excitability of new neurons may, to some extent, be specific to running conditions.

Running also resulted in changes in the subcortical projections to new neurons. While the traced cell number in the nucleus of the diagonal band of Broca remained unaltered, the ratio of traced to starter cells decreased with running, suggesting that this nucleus provides synaptic input to newborn neurons from a limited population of cells. However, the number of traced cells in the medial septum, a structure considered essential for generating and pacing theta-band oscillations throughout the hippocampal formation (Barry et al., 2012), was upregulated by exercise in proportion to the starter cells. The medial septum may be recruited to maintain the cholinergic input (Vivar et al., 2012) onto the increased number of newborn neurons generated by running. This cholinergic input may enhance intrinsic excitability of adult-born neurons by lowering the action potential threshold and inducing synaptic potential-spike coupling to allow for efficient information transfer to post-synaptic neurons (Martinello et al., 2015).

A large running-induced increase of subcortical innervation was observed for the number of medial mammillary nuclei (MM) and the supramammillary nucleus (SUM) pars lateralis cells. Indeed, these are the only brain regions where the ratio of traced cells to starter cells was significantly increased with running (Fig. 8). The specific role of MM and SUM cells projecting onto newborn GCs is still unclear. It is known that SUM pars lateralis innervates the dorsal DG and CA2/CA3 areas, and to a lesser extent, the ventral DG (Vertes and McKenna, 2000). SUM neurons fire in synchrony with the hippocampal theta rhythm (Thinschmidt et al., 1995), and appear to be directly involved in the generation of the theta rhythm (Vertes et al., 2004). Therefore, the increased integration of the SUM cells into new GC circuitry may have an important role in the generation of DG theta rhythms to improve memory function. The MM is considered important for spatial working memory, receives direct innervation from prefrontal cortex, entorhinal cortex and the subiculum and projects to the thalamus (Vann, 2010; Dillingham et al., 2015). In addition, in humans, this nucleus is atrophied in the amnesic Korsakoff's syndrome (Kopelman, 1995) and in other forms of dementia (Hornberger et al., 2012). Interestingly, no projections from MM to the hippocampus have been described previously. Future studies will be needed to elucidate the specific role of MM in new neuron circuitry.

The running induced recruitment of innervation from subcortical brain regions (MS, MM, SUM), that are important for spatial information processing and for genesis of the hippocampal theta rhythm, is complemented by increased input from caudo-medial and medial entorhinal cortex to new neurons. These entorhinal cortices contain cells that convey spatial or motion related signals such as grid, boundary, and head direction cells, which may facilitate integration of the spatial context of an experience in the hippocampus (Knierim et al., 2013; Knierim, 2015) as well as context invariant speed cells (Kropff et al., 2015). The caudo-medial entorhinal cortex projects to the septal pole of the dentate gyrus (Dolorfo and Amaral, 1998) and contributes both to spatial and recollection memory (Sauvage et al., 2010). Furthermore, the medial entorhinal cortex grid cells are considered to fire during specific phases of the theta rhythm, linked to the geometric representation of space in the hippocampus (Strange et al., 2014; Burgalossi and Brecht, 2014). The increased contribution of these areas to new neuron circuitry may explain in part the improved spatial memory function that is observed with exercise (Voss et al., 2013; Vivar et al., 2013; Patten et al., 2015). Ablation of new neurons in running mice abolishes such improvements (Clark et al.,

2008) possibly due to the loss of the cells as well as the circuitry relevant to spatial encoding in the dentate gyrus. Indeed, future studies recording from or silencing the relevant inputs that were modified by running, in conjunction with behavioral testing, may provide insight into their functional significance.

Running also increased the input from lateral entorhinal cortex (LEC) to new hippocampal neurons. In addition, paired-pulse facilitation following activation of the lateral perforant pathway was elevated by running. These changes may enhance the functional contribution of LEC inputs to newborn granule cells and support the improved pattern separation observed with exercise (Creer et al., 2010; Bolz et al., 2015). Consistently, an exercise intervention in aged humans bolstered recognition memory and early recall for complex spatial objects (Maass et al., 2015). Interestingly, we also observed sparse input from the sensory cortices to the new neurons in controls and runners. It is unclear what the significance is of these visual, auditory and somatosensory inputs. In visual cortex these cells were located in V1 and V2, important for color detection (Shapley and Hawken, 2011). In a recent study in which rats sustained lesions of the dorsal dentate gyrus a deficit in color-context pattern separation was observed (Musso and Kesner, 2015). Future studies utilizing in vivo recordings may be able to further elucidate the type of sensory information (Velez-Fort et al., 2014) that is conveyed to new neurons.

Adult neurogenesis is a process that continues throughout the lifespan. It has, however, proven challenging to elucidate the precise functional significance of this phenomenon (Marín-Burgin and Schinder, 2012; Groves et al., 2013). It could be that in sedentary subjects the newly born neurons are not optimally integrated for fine discrimination processes. Indeed, distinct storage of novel contextual and episodic information is critical for minimizing memory overlap between closely similar stimuli and events. Dentate granule cells outnumber entorhinal cells resulting in sparse encoding (Treves and Rolls, 1992; Knierim and Neunuebel, 2015) considered to underlie pattern separation (Gilbert et al., 2001; Leutgeb et al., 2007). Running may promote sparse encoding by a larger spread of incoming data over individual neurons. Enhanced distribution of incoming information over a larger population of granule cells may also provide more structural redundancy and protection from brain injury or disease (Kitano, 2004; Kaiser et al., 2007; Hütt et al., 2014). Furthermore, the running-induced recruitment of brain areas providing specific types of information, such as contextual encoding from LEC together several brain regions important for spatial-temporal memory formation (CEnt, MM, SUM, MS) may allow for a more complete integration of the new neurons into the circuitry. Interestingly, the entorhinal, mammillary and septal brain areas that provide input to new neurons are considered particularly vulnerable to aging-related dementias and neurodegenerative disease (Hyman et al., 1984; Kopelman, 1995; Hornberger et al., 2012). Running-induced network expansion may help delay or prevent the onset of such conditions. Altogether, our findings suggest that the benefits of exercise for cognition are supported not only by a local increase in new hippocampal neurons but also by changes in their afferent circuitry.

Supplementary Material

Refer to Web version on PubMed Central for supplementary material.

Acknowledgments

This work was supported by the National Institute on Aging, Intramural Research Program. We are most grateful to Linda R. Kitabayashi for her help with preparation of photomicrographs, Galit Benoni for help with the graphical abstract, Jason Boulter for technical assistance and Drs. Peter Clark, Jim Knierim, Hyo Youl Moon and Nirmath Sah for comments on the manuscript.

References

- Altman J, Das GD. Autoradiographic and histological evidence of postnatal hippocampal neurogenesis in rats. *J Comp Neurol*. 1965; 124:319–335. [PubMed: 5861717]
- Amaral DG, Witter MP. The three-dimensional organization of the hippocampal formation: a review of anatomical data. *Neuroscience*. 1995; 31:571–591. [PubMed: 2687721]
- Barry C, et al. Possible role of acetylcholine in regulating spatial novelty effects on theta rhythm and grid cells. *Front Neural Circ*. 2012; 6:5.
- Bergami M, et al. A critical period for experience-dependent remodeling of adult-born neuron connectivity. *Neuron*. 2015; 85:710–717. [PubMed: 25661179]
- Blasco-Ibañez JM, Freund TF. Distribution, ultrastructure, and connectivity of calretinin-immunoreactive mossy cells of the mouse dentate gyrus. *Hippocampus*. 1997; 7:307–320. [PubMed: 9228528]
- Bolz L, et al. Running improves pattern separation during novel object recognition. *Brain Plast*. 2015; 1:129–141. [PubMed: 29765837]
- Burgalossi A, Brecht M. Cellular, columnar and modular organization of spatial representations in medial entorhinal cortex. *Curr Opin Neurobiol*. 2014; 24(1):47–54. [PubMed: 24492078]
- Buzsáki G, Moser EI. Memory, navigation and theta rhythm in the hippocampal–entorhinal system. *Nat Neurosci*. 2013; 16:130–138. [PubMed: 23354386]
- Cenquizca LA, Swanson LW. Spatial organization of direct hippocampal field CA1 axonal projections to the rest of the cerebral cortex. *Brain Res Rev*. 2007; 56:1–26. [PubMed: 17559940]
- Clark PJ, et al. Intact neurogenesis is required for benefits of exercise on spatial memory but not motor performance or contextual fear conditioning in C57BL/6J mice. *Neuroscience*. 2008; 155:1048–1058. [PubMed: 18664375]
- Clelland CD, et al. A functional role for adult hippocampal neurogenesis in spatial pattern separation. *Science*. 2009; 325:210–213. [PubMed: 19590004]
- Creer DJ, et al. Running enhances spatial pattern separation in mice. *Proc Natl Acad Sci U S A*. 2010; 107:2367–2372. [PubMed: 20133882]
- Deshpande A, et al. Retrograde monosynaptic tracing reveals the temporal evolution of inputs onto new neurons in the adult dentate gyrus and olfactory bulb. *Proc Natl Acad Sci U S A*. 2013; 110:E1152–E1161. [PubMed: 23487772]
- Dillingham CM, et al. How do mammillary body inputs contribute to anterior thalamic function? *Neurosci Biobehav Rev*. 2015; 54:108–119. [PubMed: 25107491]
- Dolorfo CL, Amaral DG. Entorhinal cortex of the rat: organization of intrinsic and extrinsic connections. *J Comp Neurol*. 1998; 398:49–82. [PubMed: 9703027]
- Donnelly JE, et al. Physical Activity Across the Curriculum (PAAC): a randomized controlled trial to promote physical activity and diminish overweight and obesity in elementary school children. *Prev Med*. 2009; 49:336–341. [PubMed: 19665037]
- Erickson KI, et al. Exercise training increases size of hippocampus and improves memory. *Proc Natl Acad Sci U S A*. 2011; 108:3017–3022. [PubMed: 21282661]
- Eriksson PS, et al. Neurogenesis in the adult human hippocampus. *Nat Med*. 1998; 4:1313–1317. [PubMed: 9809557]
- Fanselow MS, Dong HW. Are the dorsal and ventral hippocampus functionally distinct structures? *Neuron*. 2010; 65:7–19. [PubMed: 20152109]
- Finnegan R, Becker S. Neurogenesis paradoxically decreases both pattern separation and memory interference. *Front Syst Neurosci*. 2015; 9:136. [PubMed: 26500511]

- Freund TF, Buzsáki G. Interneurons of the hippocampus. *Hippocampus*. 1996; 6:347–470. [PubMed: 8915675]
- Gilbert PE, et al. Dissociating hippocampal subregions: double dissociation between dentate gyrus and CA1. *Hippocampus*. 2001; 11:626–636. [PubMed: 11811656]
- Groves JO, et al. Ablating adult neurogenesis in the rat has no effect on spatial processing: evidence from a novel pharmacogenetic model. *PLoS Genet*. 2013; 9(9)
- Guo W, et al. Ablation of Fmrp in adult neural stem cells disrupts hippocampus-dependent learning. *Nat Med*. 2011; 17:559–565. [PubMed: 21516088]
- Haas DL, et al. Critical factors influencing stable transduction of human CD34(+) cells with HIV-1-derived lentiviral vectors. *Mol Ther*. 2000; 2:71–80. [PubMed: 10899830]
- Han ZS, et al. A high degree of spatial selectivity in the axonal and dendritic domains of physiologically identified local-circuit neurons in the dentate gyrus of the rat hippocampus. *Eur J Neurosci*. 1993; 5:395–410. [PubMed: 8261117]
- Hornberger M, et al. In vivo and post-mortem memory circuit integrity in frontotemporal dementia and Alzheimer's disease. *Brain*. 2012; 135(Pt 10):3015–3025. [PubMed: 23012333]
- Hütt MT, et al. Perspective: network-guided pattern formation of neural dynamics. *Philos Trans R Soc Lond B Biol Sci*. 2014; 369:1653. pii: 20130522.
- Hyman BT, et al. Alzheimer's disease: cell-specific pathology isolates the hippocampal formation. *Science*. 1984; 225:1168–1170. [PubMed: 6474172]
- Jinno S. Topographic differences in adult neurogenesis in the mouse hippocampus: a stereology-based study using endogenous markers. *Hippocampus*. 2011; 21:467–480. [PubMed: 20087889]
- Kaiser M, et al. Simulation of robustness against lesions of cortical networks. *Eur J Neurosci*. 2007; 25(10):3185–3192. [PubMed: 17561832]
- Kitano H. Biological robustness. *Nat Rev Genet*. 2004; 5(11):826–837. [PubMed: 15520792]
- Knierim JJ. From the GPS to HM: place cells, grid cells, and memory. *Hippocampus*. 2015:1–7. [PubMed: 25112659]
- Knierim JJ, Neunuebel JP. Tracking the flow of hippocampal computation: pattern separation, pattern completion, and attractor dynamics. *Neurobiol Learn Mem*. 2015 pii: S1074-7427(15)00188-4.
- Knierim JJ, et al. Functional correlates of the lateral and medial entorhinal cortex: objects, path integration and local–global reference frames. *Philos Trans R Soc Lond B Biol Sci*. 2013; 369(1635):20130369. [PubMed: 24366146]
- Kopelman MD. The Korsakoff syndrome. *Br J Psychiatry*. 1995; 166:154–173. [PubMed: 7728359]
- Kropff E, et al. Speed cells in the medial entorhinal cortex. *Nature*. 2015; 523:419–429. [PubMed: 26176924]
- Larson EB, et al. Exercise is associated with reduced risk for incident dementia among persons 65 years of age and older. *Ann Intern Med*. 2006; 144:73–81. [PubMed: 16418406]
- Lautenschlager NT, et al. Effect of physical activity on cognitive function in older adults at risk for Alzheimer disease: a randomized trial. *JAMA*. 2008; 300:1027–1037. [PubMed: 18768414]
- Leutgeb JK, et al. Pattern separation in the dentate gyrus and CA3 of the hippocampus. *Science*. 2007; 315:961–966. [PubMed: 17303747]
- Lewis PF, Emerman M. Passage through mitosis is required for oncoretroviruses but not for the human immunodeficiency virus. *J Virol*. 1994; 68:510–516. [PubMed: 8254763]
- Li XG, et al. The hippocampal CA3 network: an in vivo intracellular labeling study. *J Comp Neurol*. 1994; 339:181–208. [PubMed: 8300905]
- Lisman JE. Relating hippocampal circuitry to function: recall of memory sequences by reciprocal dentate–CA3 interactions. *Neuron*. 1999; 22:233–242. [PubMed: 10069330]
- Lisman JE, et al. Recall of memory sequences by interaction of the dentate and CA3: a revised model of the phase precession. *Neural Netw*. 2005; 18:1191–1201. [PubMed: 16233972]
- Lowe A, et al. Neurogenesis and precursor cell differences in the dorsal and ventral adult canine hippocampus. *Neurosci Lett*. 2015; 593:107–113. [PubMed: 25778416]
- Maass, A., et al. Vascular hippocampal plasticity after aerobic exercise in older adults. *Mol Psychiatry*. 2015. <http://dx.doi.org/10.1038/mp.2014.114>

- Marín-Burgin A, Schinder AF. Requirement of adult-born neurons for hippocampus-dependent learning. *Behav Brain Res.* 2012; 227:391–399. [PubMed: 21763727]
- Marín-Burgin A, et al. Unique processing during a period of high excitation/inhibition balance in adult-born neurons. *Science.* 2012; 335:1238–1242. [PubMed: 22282476]
- Marr D. Simple memory: a theory for archicortex. *Proc R Soc Lond B Biol Sci.* 1971; 262:23–81.
- Martinello K, et al. Cholinergic afferent stimulation induces axonal function plasticity in adult hippocampal granule cells. *Neuron.* 2015; 85:346–363. [PubMed: 25578363]
- McAvoy K, et al. Adult hippocampal neurogenesis and pattern separation in DG: a role for feedback inhibition in modulating sparseness to govern population-based coding. *Front Syst Neurosci.* 2015; 9:120. [PubMed: 26347621]
- Musso N, Kesner R. A role for the dorsal dentate gyrus in color context pattern separation. *Neurology.* 2015; S49:001.
- Nakashiba T, et al. Young dentate granule cells mediate pattern separation, whereas old granule cells facilitate pattern completion. *Cell.* 2012; 149:188–201. [PubMed: 22365813]
- Niibori Y, et al. Suppression of adult neurogenesis impairs population coding of similar contexts in hippocampal CA3 region. *Nat Commun.* 2012; 3:1253. <http://dx.doi.org/10.1038/ncomms2261>. [PubMed: 23212382]
- Nowakowski RS, Rakic P. The site of origin and route and rate of migration of neurons to the hippocampal region of the rhesus monkey. *J Comp Neurol.* 1981; 196:129–154. [PubMed: 7204662]
- Patten AR, et al. The benefits of exercise on structural and functional plasticity in the rodent hippocampus of different disease models. *Brain Plast.* 2015; 1:97–127. [PubMed: 29765836]
- Paxinos, G., Franklin, K. *Mouse Brain in Stereotaxic Coordinates.* Academic Press; 2007.
- Pereira AC, et al. An in vivo correlate of exercise-induced neurogenesis in the adult dentate gyrus. *Proc Natl Acad Sci U S A.* 2007; 104:5638–5643. [PubMed: 17374720]
- Piatti VC, et al. The timing for neuronal maturation in the adult hippocampus is modulated by local network activity. *J Neurosci.* 2011; 31:7715–7728. [PubMed: 21613484]
- Sahay A, Hen R. Adult hippocampal neurogenesis in depression. *Nat Neurosci.* 2007; 10:1110–1115. [PubMed: 17726477]
- Sahay A, et al. Pattern separation: a common function for new neurons in hippocampus and olfactory bulb. *Neuron.* 2011a; 70:582–588. [PubMed: 21609817]
- Sahay A, et al. Increasing adult hippocampal neurogenesis is sufficient to improve pattern separation. *Nature.* 2011b; 472:466–470. [PubMed: 21460835]
- Sauvage MM, et al. The caudal medial entorhinal cortex: a selective role in recollection-based recognition memory. *J Neurosci.* 2010; 30:15695–15699. [PubMed: 21084625]
- Scharfman HE. The CA3 “backprojection” to the dentate gyrus. *Prog Brain Res.* 2007; 163:627–637. [PubMed: 17765742]
- Schmidt-Hieber C, et al. Enhanced synaptic plasticity in newly generated granule cells of the adult hippocampus. *Nature.* 2004; 429:184–187. [PubMed: 15107864]
- Shapley R, Hawken MJ. Color in the cortex: single- and double-opponent cells. *Vis Res.* 2011:701–717. [PubMed: 21333672]
- Sleiman SF, Chao MV. Downstream consequences of exercise through the action of BDNF. *Brain Plast.* 2015; 1:143–148. [PubMed: 29765838]
- Snyder JS, et al. Anatomical gradients of adult neurogenesis and activity: young neurons in the ventral dentate gyrus are activated by water maze training. *Hippocampus.* 2009; 19:360–370. [PubMed: 19004012]
- Strange BA, et al. Functional organization of the hippocampal longitudinal axis. *Nat Rev Neurosci.* 2014; 15:655–669. [PubMed: 25234264]
- Tanti A, et al. Differential environmental regulation of neurogenesis along the septo-temporal axis of the hippocampus. *Neuropharmacology.* 2012; 63:374–384. [PubMed: 22561281]
- Tashiro A, et al. NMDA-receptor-mediated, cell-specific integration of new neurons in adult dentate gyrus. *Nature.* 2006; 442:929–933. [PubMed: 16906136]

- Temprana SG, et al. Delayed coupling to feedback inhibition during a critical period for the integration of adult-born granule cells. *Neuron*. 2015; 85:116–130. [PubMed: 25533485]
- Thinschmidt JS, et al. The supramammillary nucleus: is it necessary for the mediation of hippocampal theta rhythm? *Neuroscience*. 1995; 67:301–312. [PubMed: 7675171]
- Treves A, Rolls ET. Computational constraints suggest the need for two distinct input systems to the hippocampal CA3 network. *Hippocampus*. 1992; 2:189–199. [PubMed: 1308182]
- Treves A, et al. What is the mammalian dentate gyrus good for? *Neuroscience*. 2008; 154:1155–1172. [PubMed: 18554812]
- Tronel S, et al. Adult-born neurons are necessary for extended contextual discrimination. *Hippocampus*. 2012; 22:292–298. [PubMed: 21049483]
- Van der Borght K, et al. Exercise improves memory acquisition and retrieval in the Y-maze task: relationship with hippocampal neurogenesis. *Behav Neurosci*. 2007; 121:324–334. [PubMed: 17469921]
- van Groen T. Entorhinal cortex of the mouse: cytoarchitectonical organization. *Hippocampus*. 2001; 11:397–407. [PubMed: 11530844]
- van Praag H, et al. Running increases cell proliferation and neurogenesis in the adult mouse dentate gyrus. *Nat Neurosci*. 1999a; 2:266–270. [PubMed: 10195220]
- van Praag H, et al. Running enhances neurogenesis, learning, and long-term potentiation in mice. *Proc Natl Acad Sci U S A*. 1999b; 96:13427–13431. [PubMed: 10557337]
- van Praag H, et al. Functional neurogenesis in the adult hippocampus. *Nature*. 2002; 415:1030–1034. [PubMed: 11875571]
- Vann SD. Re-evaluating the role of the mammillary bodies in memory. *Neuropsychologia*. 2010; 48:2316–2327. [PubMed: 19879886]
- Velez-Fort M, et al. The stimulus selectivity and connectivity of layer six principal cells reveals cortical microcircuits underlying visual processing. *Neuron*. 2014; 17:1431–1443.
- Vertes RP, McKenna JT. Collateral projections from the supramammillary nucleus to the medial septum and hippocampus. *Synapse*. 2000; 38:281–293. [PubMed: 11020231]
- Vertes RP, et al. Theta rhythm of the hippocampus: subcortical control and functional significance. *Behav Cogn Neurosci Rev*. 2004; 3:173–200. [PubMed: 15653814]
- Vivar C, van Praag H. Functional circuits of new neurons in the dentate gyrus. *Front Neural Circ*. 2013; 7:15.
- Vivar C, et al. Monosynaptic inputs to new neurons in the dentate gyrus. *Nat Commun*. 2012; 3:1107. [PubMed: 23033083]
- Vivar C, et al. All about running: synaptic plasticity, growth factors and adult hippocampal neurogenesis. *Curr Top Behav Neurosci*. 2013; 15:189–210. [PubMed: 22847651]
- Voss MW, et al. Bridging animal and human models of exercise-induced brain plasticity. *Trends Cogn Sci*. 2013; 17:525–544. [PubMed: 24029446]
- Wickersham IR, et al. Monosynaptic restriction of transsynaptic tracing from single, genetically target neurons. *Neuron*. 2007; 53:639–647. [PubMed: 17329205]
- Yassa MA, Stark CE. Pattern separation in the hippocampus. *Trends Neurosci*. 2011; 34(1.0):515–525. [PubMed: 21788086]
- Zhang W, et al. Surviving hilar somatostatin interneurons enlarge, sprout axons, and form new synapses with granule cells in a mouse model of temporal lobe epilepsy. *J Neurosci*. 2009; 29:14247–14256. [PubMed: 19906972]
- Zhao C, et al. Distinct morphological stages of dentate granule neuron maturation in the adult mouse hippocampus. *J Neurosci*. 2006; 26:3–11. [PubMed: 16399667]

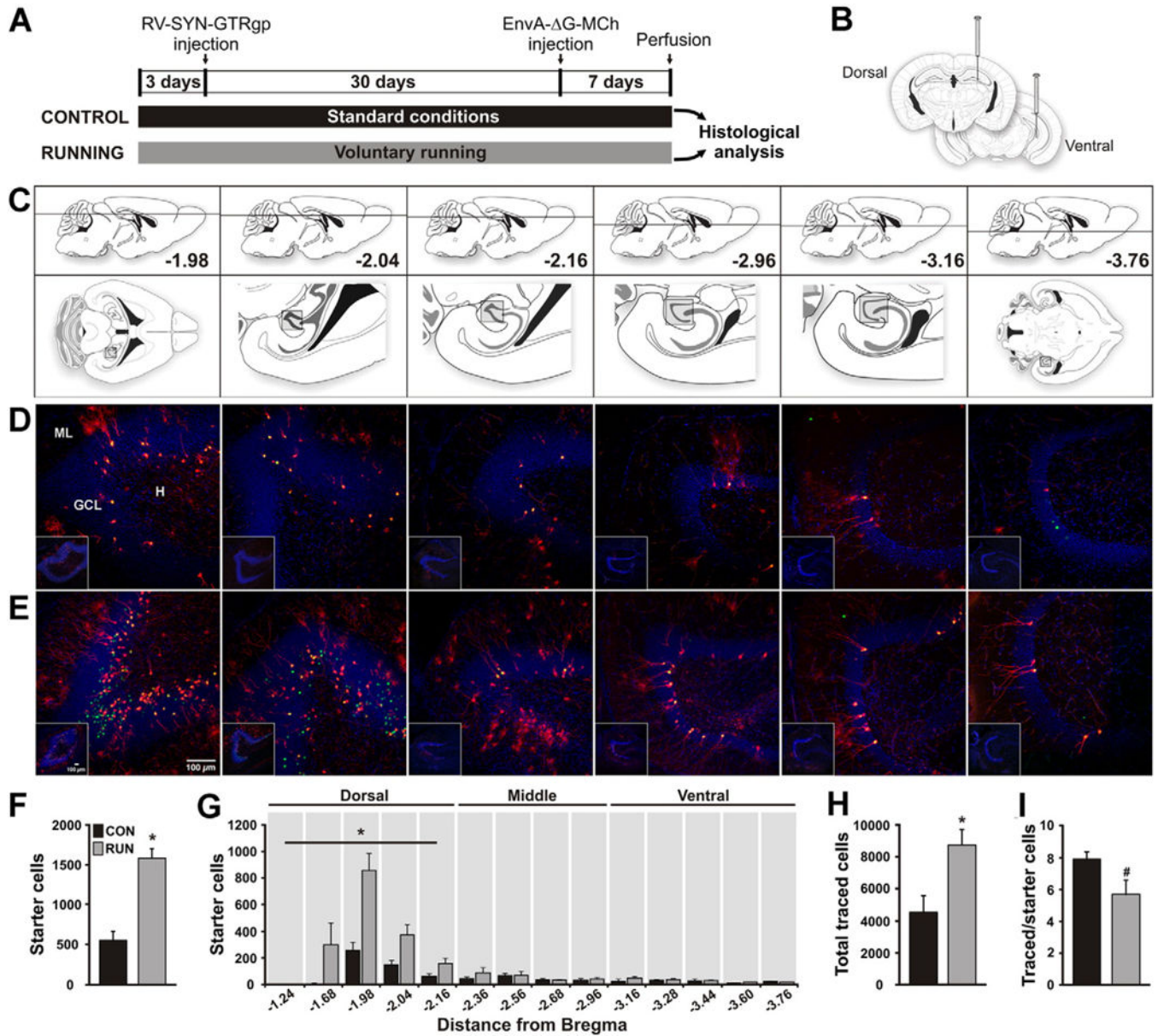


Fig. 1. Running increases the number of newborn granule cells (GCs) in the adult mouse dentate gyrus (DG) and modifies their inputs. (A) Timeline of the experiment. (B) To label dividing cells control (CON) and running (RUN) mice were injected with retrovirus expressing nuclear GFP, avian TVA receptor and rabies glycoprotein (RV-SYN-GTRgp) into the dorsal and ventral DG. After a one month interval, to allow progenitors to differentiate into new neurons, EnvA-pseudotyped rabies virus expressing MCh (EnvA- G-MCh) was injected into the same sites to trace afferent inputs to newborn GCs. (C) Modified mouse brain atlas (Paxinos and Franklin, 2007) images. Upper panels show the dorso-ventral horizontal section depth (distance from Bregma). Lower panels show overviews of horizontal sections, with the boxed areas corresponding to the DG area shown in the insets in the photomicrographs below. (D, E) Horizontal sections derived from (D) CON and (E) RUN

mice. Photomicrographs showing GFP⁺-MCh⁺ double labeled cells (green and red = yellow nuclei and red cytoplasm), called starter cells (SC), and MCh⁺ (red) traced cells (TC) throughout the dorso-ventral extent of the DG. Insets show low power DG overviews, corresponding to the boxed areas (C) in the atlas. (F) Running significantly increases SC number ($t_{(11)} = 6.15$, $P < 0.0001$; CON $n = 6$, RUN $n = 7$). (G) Dorsal to ventral distribution of SC throughout the extent of the DG. Running significantly increases the number of SC in the dorsal DG (CON, 392 ± 79 vs RUN, 1310 ± 123 ; $t_{(11)} = 6.47$, $P < 0.0001$), but not the middle or ventral DG (middle; CON, 106 ± 32 vs RUN, 148 ± 46 , $t_{(11)} = 0.46$, $P = 0.66$; ventral: CON, 68 ± 19 vs RUN, 100 ± 21 , $t_{(11)} = 0.9$, $P = 0.39$). (H) TC number is significantly increased in RUN mice ($t_{(11)} = 2.89$; $P < 0.02$; CON $n = 6$, RUN $n = 7$). (I) The TC to SC ratio shows a trend towards a decrease in RUN mice as compared to CON mice ($t_{(11)} = 2.08$; $\#P = 0.06$). Data are means \pm S.E.M. * $P < 0.05$. ML, molecular layer of the DG; GCL, granule cell layer; H, hilus. Nuclei stained with 4',6-diamidino-2-phenylindole (DAPI), blue.

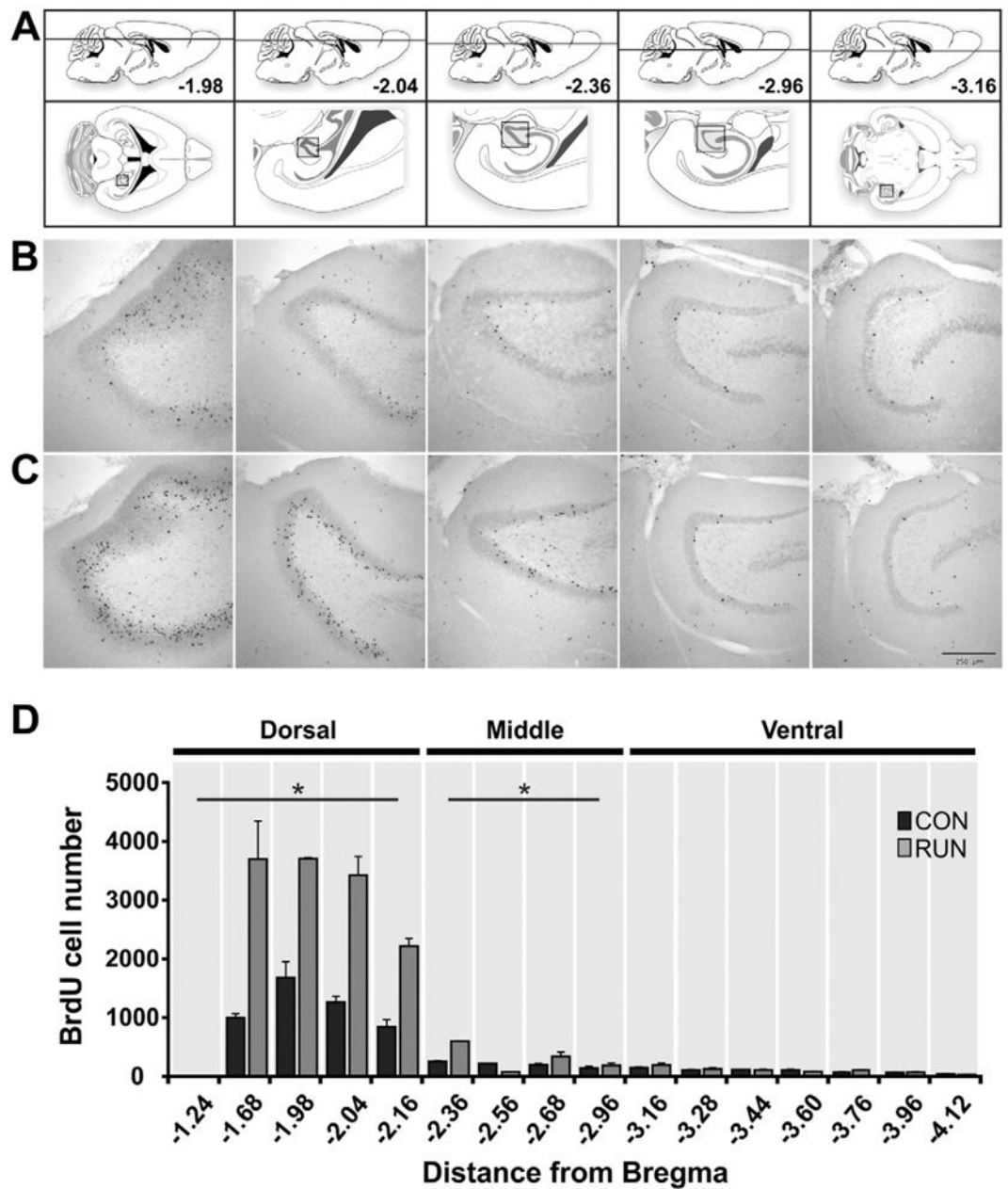


Fig. 2. Dorso-ventral distribution of bromodeoxyuridine (BrdU) labeled cells in the DG of controls and runners. (A) Modified atlas images (Paxinos and Franklin, 2007). Upper images show the dorso-ventral horizontal section depth (distance from Bregma). Lower images show an overview of the horizontal sections, with the boxed areas corresponding to the DG area in the photomicrographs below. (B, C) Photomicrographs showing BrdU⁺ cells in horizontal sections throughout the extent of the dorso-ventral DG, derived from (B) CON and (C) RUN mice. (D) Dorsal to ventral distribution of BrdU⁺ cells throughout the extent of the DG in CON ($n = 5$) and RUN ($n = 5$) mice. Running significantly increases the number of BrdU⁺ cells in the dorsal DG (CON, 2932 ± 521 vs RUN, 6694 ± 1180 ; $t_{(8)} = 2.61$, $P < 0.03$) and middle DG (CON, 535 ± 105 vs RUN, 1138 ± 194 ; $t_{(8)} = 2.44$, $P < 0.04$), but not the ventral

DG (CON, 439 ± 76 vs RUN, 515 ± 51 ; $t_{(8)} = 0.74$, $P > 0.47$) DG. Data are means \pm S.E.M.
* $P < 0.05$.

Author Manuscript

Author Manuscript

Author Manuscript

Author Manuscript

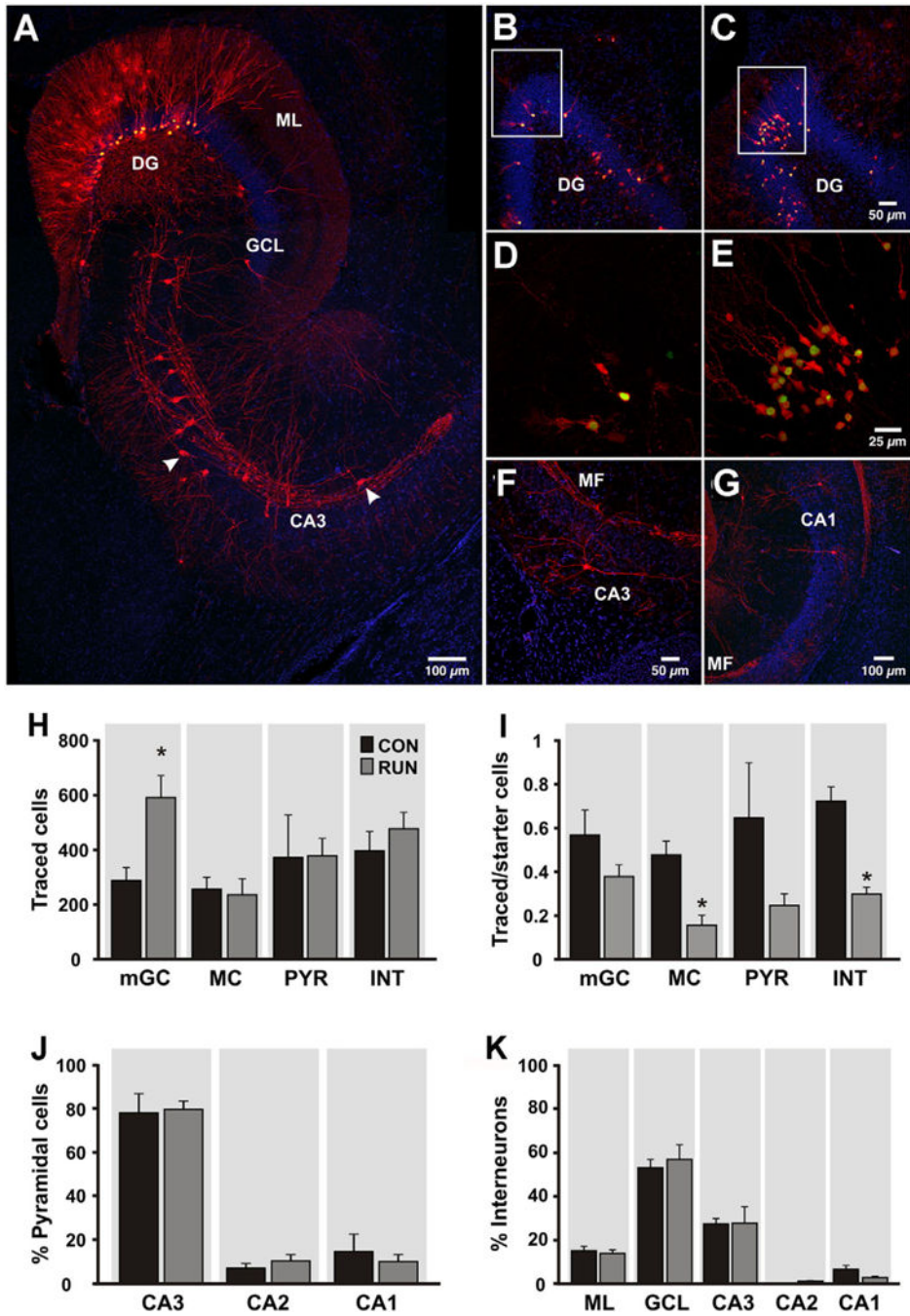


Fig. 3. Intra-hippocampal afferents to adult-born granule cells (GCs) are changed by running. (A) Horizontal section through the dentate gyrus (DG) and area CA3 derived from a runner mouse. Newborn starter cells (SC) express nuclear GFP and cytoplasmic MCh (green + red = yellow nuclei and red cytoplasm), whereas trans-synaptically traced cells (TC) express MCh only (red). Traced cells in the DG include mature granule cells (mGC), mossy cells (MC) and interneurons (INT). In area CA3, traced pyramidal cells (PYR) as well as INT (arrowheads) were observed. (B, C) Overview of DG in sections derived from (B) CON and

(C) RUN mice showing traced mGC and SC. (D, E) High power photomicrographs showing traced mGC (red) closely associated with SC (yellow nuclei) in (D) CON and (E) RUN, corresponding to the boxed areas in (B) and (C), respectively. (F) Traced INT in area CA3. (G) PYR were observed in area CA1 and (A) area CA3. (H) Quantification of traced mGC, MC, CA3–CA1 PYR and INT providing input to SC in control (CON, $n = 6$) and runner (RUN, $n = 7$) mice. Only traced mGC number was significantly increased by running ($t_{(11)} = 3.17$; $P < 0.009$). (I) Ratio of traced mGC, MC, PYR and INT to SC. The ratios of MC and INT to SC were significantly reduced by running (MC, $t_{(11)} = 4.14$, $P < 0.002$; INT, $t_{(11)} = 6.02$, $P < 0.0001$). (J) Percentage of traced PYR in areas CA3, CA2 and CA1 of the hippocampus. No difference was found between groups ($P > 0.05$). (K) Percentage of traced INT distributed in the molecular layer of the DG (ML), GC layer (GCL), and areas CA3–CA1. No difference was found between groups ($P > 0.05$). Nuclei were stained with DAPI (blue). Data are means \pm S.E.M. * $P < 0.05$.

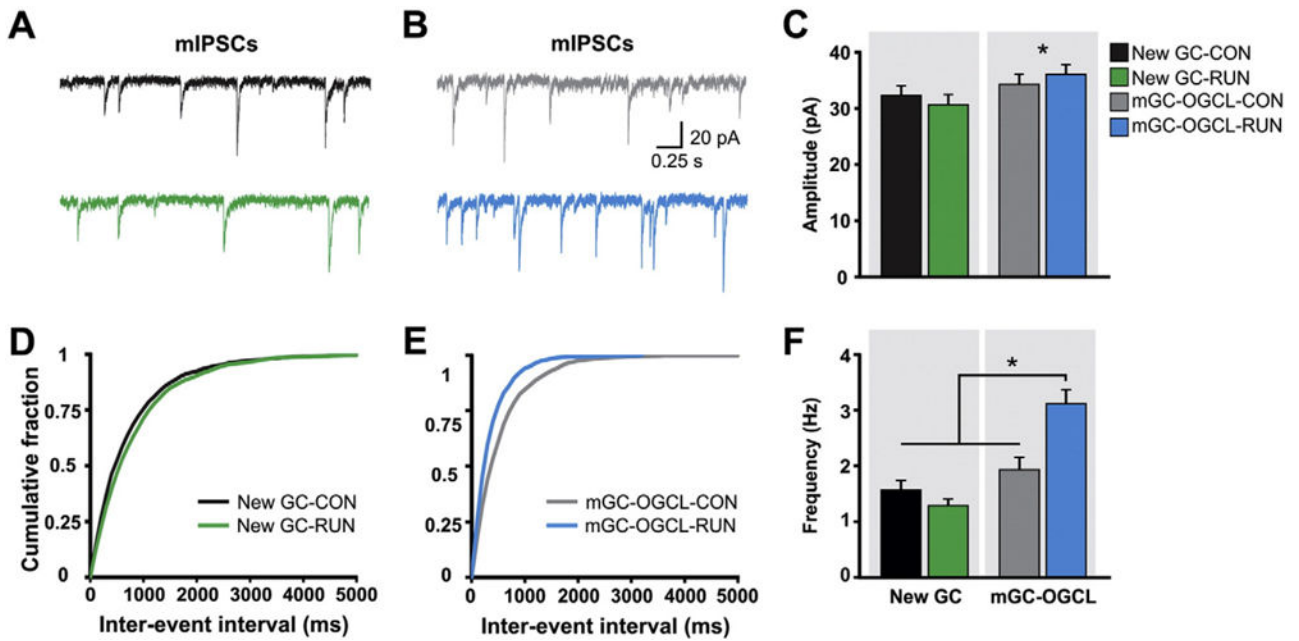


Fig. 4.

Mature GCs localized in the outer GCL (mGCs-OGCL) but not new GCs are strongly inhibited by running. (A) Example traces of whole cell patch-clamp recordings of mIPSCs from retrovirally-labeled new GCs in acute hippocampal slices derived from CON (black trace) and RUN (green trace) mice. (B) Representative mIPSCs traces from mGCs-OGCL from CON (gray trace) and RUN (blue trace) mice. (C) Summary bar graph for mean amplitude of mIPSCs from new GCs and mGCs-OGCL from CON and RUN groups. Two-way analysis of variance (ANOVA) showed that there is no interaction between GC type (new GC or mGC-OGCL) and housing (CON or RUN) condition ($F_{(1,38)} = 0.91, P > 0.34$). There is a significant main effect of cell type ($F_{(1,38)} = 4.20, P < 0.05$), indicating that mIPSC amplitude is higher in mGC-OGCL than in new GCs. (D, E) Cumulative probability plot of (D) new GCs and (E) mGCs-OGCL, mIPSCs inter-event interval in CON and RUN groups. (F) Summary bar graph for mean frequency of mIPSCs from new GCs and mGCs-OGCL. Two-way ANOVA revealed a significant interaction between cell type and housing condition ($F_{(1,38)} = 12.49, P < 0.001$). Post-hoc comparisons showed that running significantly increased the frequency of mIPSCs of mGC-OGCL as compared to all other groups ($P < 0.0002$). New GCs: CON $n = 12$ cells from 3 mice, RUN $n = 9$ cells from 4 mice; mGC-OGCL: CON $n = 10$ cells from 3 mice, RUN $n = 11$ cells from 3 mice. Data are means \pm S.E.M. * $P < 0.05$.

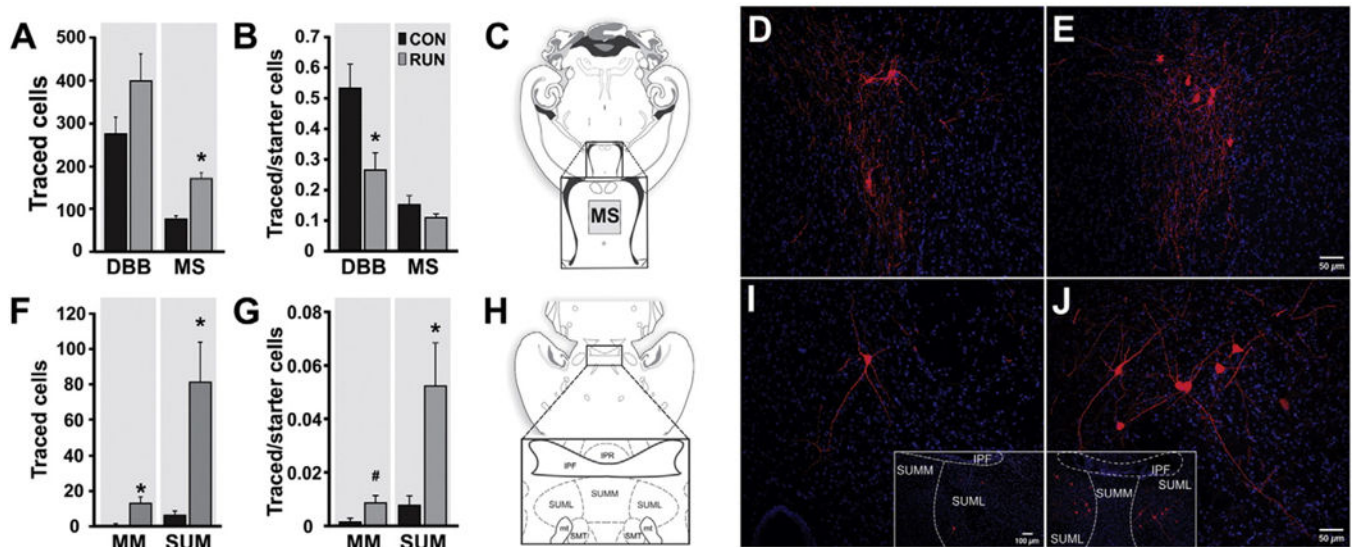
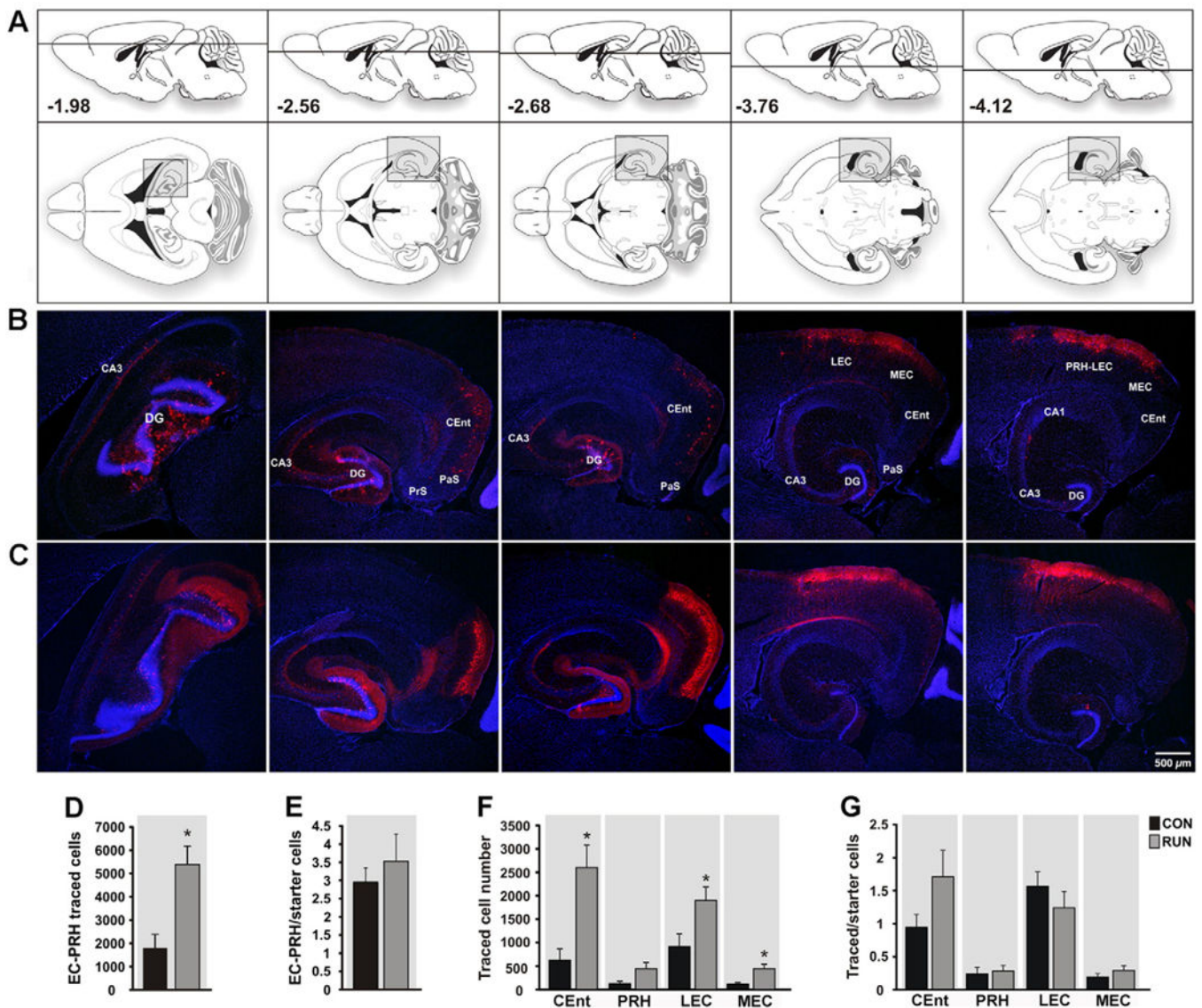


Fig. 5.

Running modifies subcortical connections to new GCs. (A) Quantification of traced cells (TC) expressing MCh (red) localized in basal forebrain [diagonal band of Broca (DBB) and medial septum (MS)] from control (CON, $n = 6$) and runner (RUN, $n = 7$) mice. Running significantly increased MS TC number ($t_{(11)} = 5.12$; $P < 0.0003$), but not DBB TC ($t_{(11)} = 1.57$, $P = 0.15$). (B) Ratio of traced DBB cells to SC was reduced by running ($t_{(11)} = 2.83$; $P < 0.016$), whereas the ratio of traced MS cells to SC was unchanged ($t_{(11)} = 1.36$, $P = 0.20$). (C) Diagram of a horizontal section (adapted from Paxinos and Franklin, 2007). The inset shows the location of traced MS cells. (D, E) Photomicrographs of traced MS cells in sections derived from (D) CON and (E) RUN mice. (F) Quantification of TC localized in medial mammillary (MM) and supramammillary nucleus (SUM) pars lateralis from CON ($n = 6$) and RUN ($n = 7$) mice. Running significantly increased the number of traced MM ($t_{(11)} = 2.66$; $P < 0.02$) and SUM cells ($t_{(11)} = 3.03$; $P < 0.01$). (G) Ratio of traced SUM cells to SC was significantly increased by running ($t_{(11)} = 2.50$; $P < 0.03$), whereas the ratio of traced MM cells to SC showed a trend towards an increase ($t_{(11)} = 2.16$; $\#P = 0.053$). (H) Diagram of a horizontal section (adapted from Paxinos and Franklin, 2007), inset shows the SUM. (I, J) Photomicrographs of sections showing traced SUM cells in sections derived from (I) CON and (J) RUN mice. SUML, supramammillary nucleus pars lateralis; SUMM, supramammillary nucleus pars medialis; IPF, interpeduncular fossa; IPR, interpeduncular nucleus; mt, mammillo-thalamic tract; SMT, sub-mammillo-thalamic nucleus. Nuclei were stained with DAPI (blue). Data are means \pm S.E.M. * $P < 0.05$.

**Fig. 6.**

Entorhinal cortex input to new GCs is reorganized by running. (A) Modified atlas plates (Paxinos and Franklin, 2007) corresponding to the photomicrographs of sections derived from (B) CON and (C) RUN mice. Upper atlas panels show the dorso-ventral horizontal section depth (distance from Bregma). The lower images show overviews of horizontal sections; shaded areas correspond to the photomicrographs below. (B, C) Photomicrographs showing traced cells (TC) in horizontal sections derived from (B) CON and (C) RUN mice. (D) The total number of TC in entorhinal–perirhinal cortex (EC–PRH) was increased by running ($t_{(11)} = 3.55$, $P < 0.004$; CON $n = 6$; RUN $n = 7$). (E) Running did not alter the ratio of total EC–PRH TC to SC ($t_{(11)} = 0.69$; $P = 0.5$). (F) Within the EC, caudo-medial entorhinal cortex (CEnt), lateral entorhinal cortex (LEC), and medial entorhinal cortex (MEC) TC number was increased by running as compared to controls (CEnt, $t_{(11)} = 3.49$, $P < 0.005$; LEC, $t_{(11)} = 2.38$, $P < 0.04$; MEC, $t_{(11)} = 3.08$, $P < 0.01$). (G) Running did not alter

the ratio of TC to SC in the peri- and entorhinal cortices ($P > 0.05$). Data are means \pm S.E.M. * $P < 0.05$. Abbreviations: parasubiculum (PaS); presubiculum (PrS).

Author Manuscript

Author Manuscript

Author Manuscript

Author Manuscript

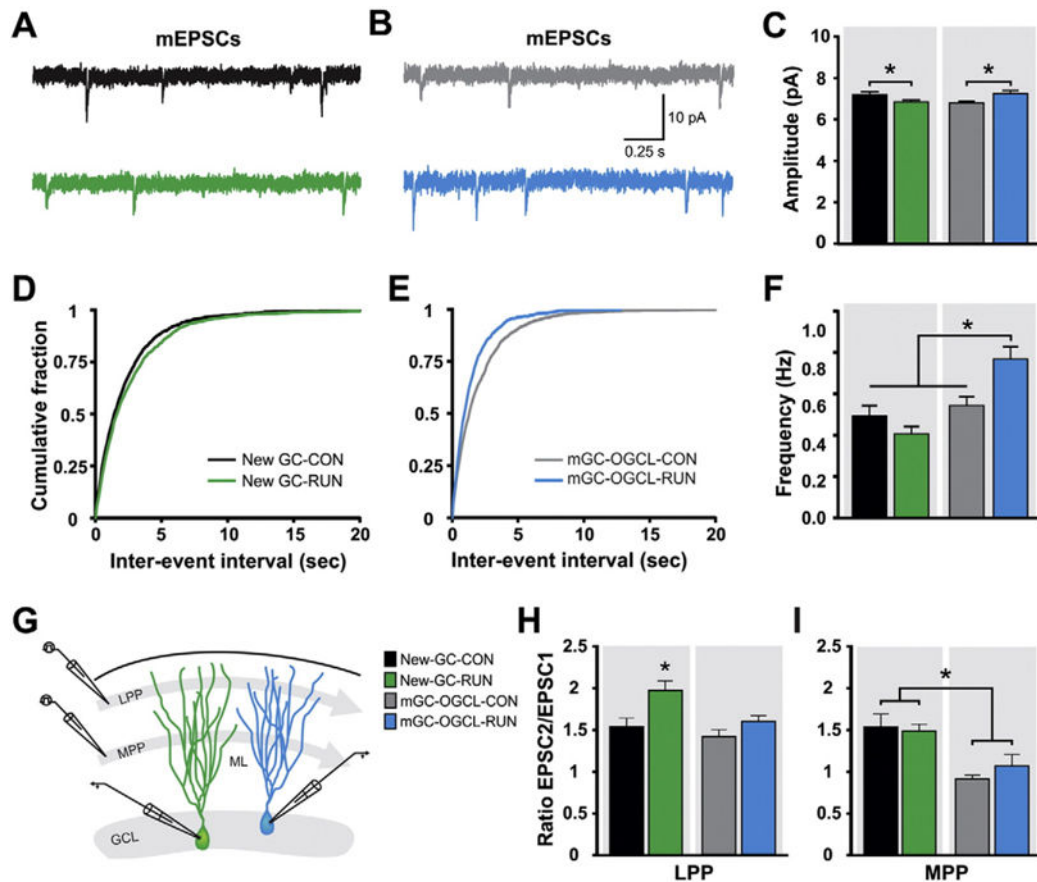


Fig. 7.

Running modifies glutamatergic synaptic transmission onto DG cells. (A, B) Representative mEPSCs traces from retrovirally labeled new GCs (A) and mGCs-OGCL (B) in acute hippocampal slices derived from CON and RUN mice [new GC: CON (black trace), RUN (green trace); mGCs-OGCL: CON (gray trace), RUN (blue trace)]. (C) Summary bar graph for mean amplitude of mEPSCs from new GCs (CON, $n = 13$ cells from 3 mice, RUN, $n = 17$ cells from 6 mice) and mGCs-OGCL (CON, $n = 18$ cells from 4 mice, RUN, $n = 10$ cells from 6 mice). Two-way ANOVA revealed a significant interaction between cell type and housing condition ($F_{(1,54)} = 13.22$, $P < 0.0006$), but no main effect of cell type ($F_{(1,54)} = 0.19$, $P > 0.89$) or housing condition ($F_{(1,54)} = 0.18$, $P > 0.67$). Running reduced the mean amplitude of mEPSCs in newborn GCs ($P < 0.02$), whereas the amplitude is increased in mGCs-OGCL ($P < 0.008$). (D, E) Cumulative probability plot of (D) new GCs and (E) mGCs-OGCL mEPSC inter-event interval from CON and RUN groups. (F) Summary bar graph for mean frequency of mEPSCs from new GCs and mGCs-OGCL from CON and RUN mice. Two-way ANOVA revealed a significant interaction between cell type and housing condition ($F_{(1,54)} = 11.09$, $P < 0.002$) and a main effect of cell type ($F_{(1,54)} = 19.8$, $P < 0.0001$), but not of housing condition ($F_{(1,54)} = 2.18$, $P > 0.15$). Running significantly increased mEPSC frequency of mGCs-OGCL compared to all other groups ($P < 0.02$). (G) Schematic representation of the stimulation of the lateral (LPP) and medial (MPP) perforant pathway in the molecular layer (ML) of the DG and recordings from new GCs (green cell) and mGC-OGCL (blue cell). (H) Summary of paired pulse ratio (PPR) of EPSCs evoked at

50 ms inter-pulse interval by stimulation of LPP from new GCs (CON, $n = 6$ cells from 5 mice, RUN $n = 8$ cells from 5 mice), and mGCs-OGCL (CON, $n = 8$ cells from 8 mice, RUN, $n = 10$ cells from 8 mice). Two-way ANOVA showed no interaction between cell type and housing condition ($F_{(1,28)} = 1.88, P > 0.18$). There are significant main effects of housing condition ($F_{(1,28)} = 11.57, P < 0.002$) and cell type ($F_{(1,28)} = 7.69, P < 0.009$). Running significantly increased paired-pulse facilitation onto new GCs compared to all other groups ($P < 0.004$). (I) Summary of PPR of EPSCs evoked by stimulation of MPP from new GCs (CON, $n = 10$ cells from 8 mice, RUN, $n = 7$ cells from 4 mice) and mGCs-OGCL (CON, $n = 11$ cells from 10 mice, RUN, $n = 6$ cells from 4 mice). Two-way ANOVA showed no interaction between cell type and housing condition ($F_{(1,30)} = 0.92, P > 0.35$). There is a significant main effect of cell type ($F_{(1,30)} = 21.04, P < 0.0001$), but not of housing condition ($F_{(1,30)} = 0.26, P > 0.6$). Data are means \pm S.E.M. * $P < 0.05$.

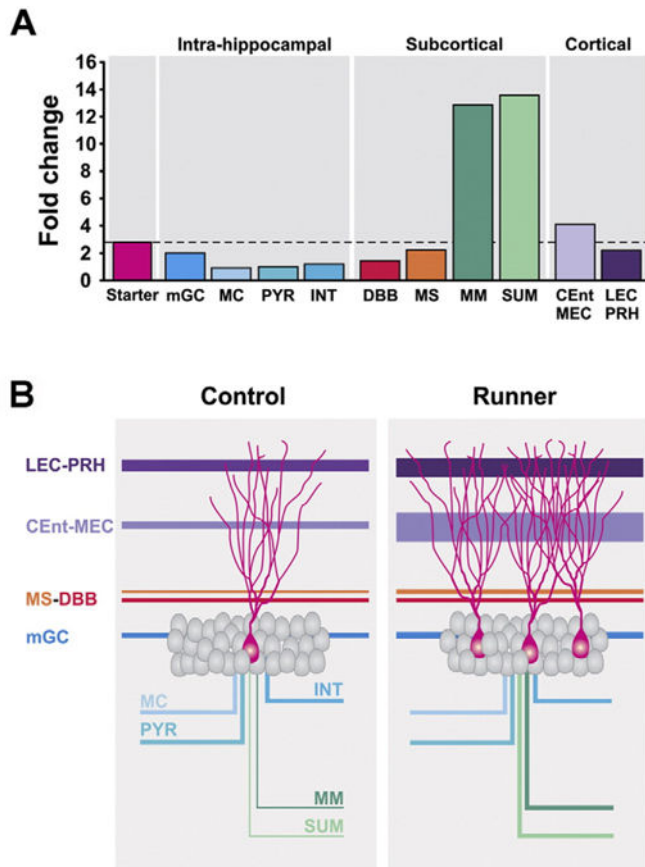


Fig. 8. Running-induced fold changes and model of the effects of running on the neuronal network of newborn GCs. (A) Running-induced fold changes in the newborn GCs (starter cells) and the synaptic inputs from intra-hippocampal, subcortical and cortical areas. Only medial mammillary (MM) and supramammillary (SUM) nuclei exceeded (~13-fold) the fold change of the starter cells (~3-fold). (B) Model showing the relative contribution of the regions that innervate new GCs under control and running conditions.